Electronic Supplementary Information

Ascorbyl and hydroxyl radical generation mediated by a copper complex adsorbed on gold

Adolfo I. B. Romo,[a] Vitória S. Dibo,[a] Dieric S. Abreu,[a,b] Marta S. P. Carepo,[a,c] Andrea C. Neira,[d] Ivan Castillo,[d] Luis Lemus,[e] Otaciro R. Nascimento,[f] Paul V. Bernhardt,[g] Eduardo H. S. Sousa,[a] Izaura C. N. Diógenes[a*]

a. *Departamento de Química Orgânica e Inorgânica, Universidade Federal do Ceará, Cx. Postal 6021, Fortaleza, CE, Brasil, 60451-970. Email: izaura@dqoi.ufc.br*
b. *Departamento de Física, Universidade Federal do Ceará, Campus do Pici, Caixa Postal 6030, Fortaleza, CE, Brasil, 60455-970.*
c. *LAQV, REQUIMTE, Departamento de Química, Faculdade de Ciências e Tecnologia, Universidade Nova de Lisboa, Caparica, Portugal.*
d. *Instituto de Química, Universidad Nacional Autónoma de México, Circuito Exterior, Ciudad Universitaria, 04510, México.*
e. *Facultad de Química y Biologia, Universidad de Santiago de Chile, Alameda 3363, Estación Central, Santiago, Chile.*
f. *Instituto de Física de São Carlos, Universidade de São Paulo, CP 369, CEP 13560-970, São Carlos, SP.*
g. *School of Chemistry and Molecular Biosciences, University of Queensland, Brisbane, 4072, Australia.*

Electron paramagnetic resonance (EPR) spectrum of $[Cu(4\text{-mbpy-Bz-SMe})_2]^{2+}$

Fig. S1 presents the EPR spectrum of $[Cu(4\text{-mbpy-Bz-SMe})_2]^{2+}$ measured as a dilute (1 mmol L^{-1}) frozen dimethylformamide (DMF) solution at 125 K.

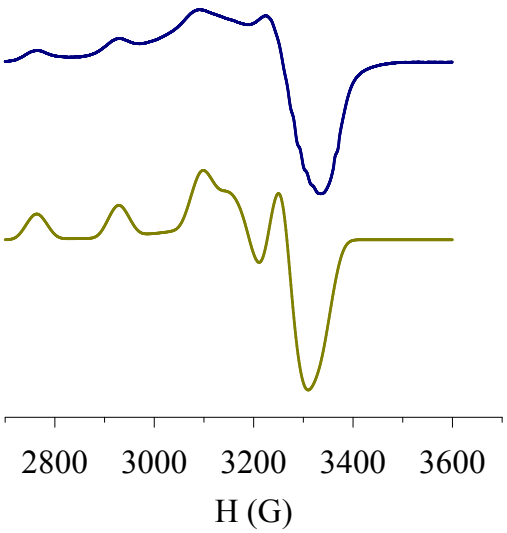

Fig. S1. Top: X-band EPR spectrum of $[Cu(4\text{-mbpy-Bz-SMe})_2]^{2+}$ (1mmol L^{-1} in DMF, 125 K). Bottom: simulated spectrum; spin Hamiltonian parameters g_x 2.065 (A_x 10 G); g_y 2.125 (A_y 40 G); g_z 2.242 (A_z 165 G) and A_N 15 G (super hyperfine coupling). The spectrum was simulated with EPR50F.[1]

Electrochemistry of $[Cu(4\text{-mbpy-Bz-SMe})_2]^{2+}$ in solution with and without oxygen

Fig. S2 shows the cyclic voltammograms obtained for a glassy carbon electrode in PBS solution containing $[Cu(4\text{-mbpy-Bz-SMe})_2]^{2+}$.

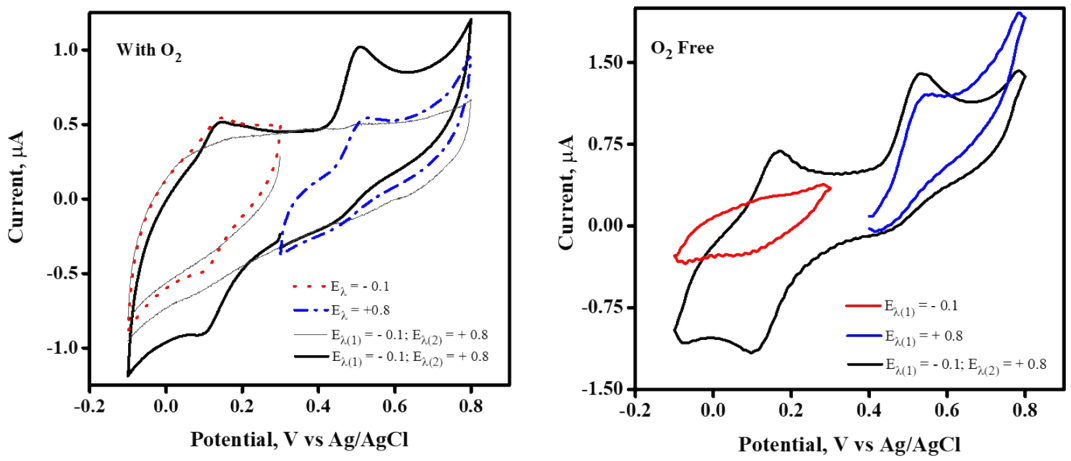

Fig. S2. Cyclic voltammograms of glassy carbon electrode at 10 mV s^{-1} in 0.1 mol L^{-1} PBS (pH 7.2) containing $[Cu(4\text{-mbpy-Bz-SMe})_2]^{2+}$ starting at +0.3V (red) and +0.4 (blue and black) and scanning in different directions as indicated by the switching potential (E_λ). For the O_2 free condition, the experiments were performed in a glovebox.

Fig. S3 presents successive spectra of $[Cu^{I}(4\text{-mbpy-Bz-SMe})_2]^{+}$ in tetrahydrofuran (THF) at different temperatures.

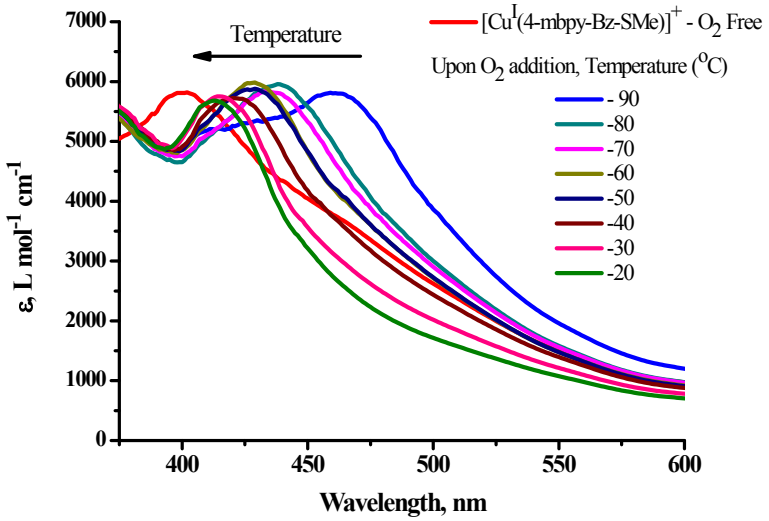

Fig. S3. UV-Vis spectra of $[Cu^{I}(4\text{-mbpy-Bz-SMe})_2]^{+}$ in tetrahydrofuran (THF) before at 183 K (red) and after oxygen addition at different temperatures as indicated in the inserted graph legend.

Gold surface modified with $[Cu(4\text{-mbpy-Bz-SMe})_2]^{2+}$

Gold polycrystalline substrates were spontaneously modified by immersing in ethanolic solution containing 10.0 μmol L^{-1} of $[Cu(4\text{-mbipy-Bz-SMe})_2]^{2+}$ thus forming the Au/[Cu] electrode. The reductive desorption of $[Cu(4\text{-mbpy-Bz-SMe})_2]^{2+}$ from the gold surface was performed by linear sweep voltammogram (LSV) in alkaline medium and is shown in Fig. S4.

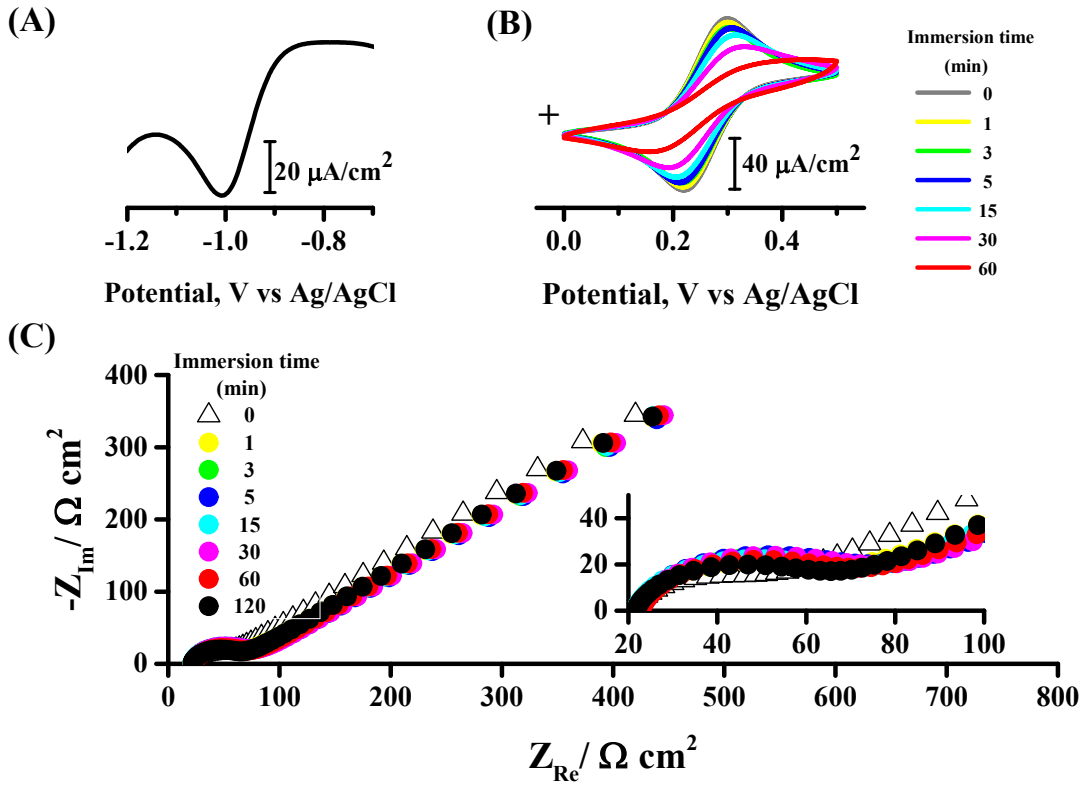

Fig. S4. (A) Linear sweep voltammogram of the modified gold electrode (1 h of immersion) at 0.1 V s^{-1} in 0.5 mol L^{-1} KOH. (B) Cyclic voltammograms at 0.1 V s^{-1} and (C) Nyquist diagrams in 0.1 mol L^{-1} KF containing 5.0 mmol L^{-1} $[Fe(CN)_6]^{3-/4-}$ in function of the immersion time of the gold electrode in 10.0 μmol L^{-1} solution of $[Cu(4\text{-mbipy-Bz-SMe})_2]^{2+}$. Inset in (C): Nyquist diagrams in the region from 0 to 100 Ω cm^2.

The cyclic voltammograms and Nyquist diagrams illustrated in Fig. S3 (B) and (C), respectively, were acquired in KF solution containing $[Fe(CN)_6]^{3-/4-}$ as a redox probe species aiming to evaluate the packing density of the SAM formed with $[Cu(4\text{-mbipy-Bz-SMe})_2]^{2+}$ on gold. The surface coverage (θ) and the electron transfer rate constant (k_{app}) of the redox probes were calculated from the Nyquist diagrams according to Equations 1 and 2:

$$\theta = 1 - \left(\frac{R_{CT}}{R_{CT}^{*}}\right) \quad (1)$$

$$k_{app} = {RT}/{F^2 R_{CT}^{*} C^{*}} \quad (2)$$

where R_{ct} and R^*_{CT} are the charge-transfer resistances for the bare and modified gold electrodes, respectively, and C* is the concentration of the redox probe in the bulk solution. The impedimetric parameters obtained in function of the immersion time are displayed in Table S1.

Table S1. Values of charge transfer resistance (R^*_{CT}), fractional coverage (θ), and apparent charge-transfer rate constant (k_{app}) of $[Fe(CN)_6]^{3-/4-}$ as a function of the immersion time of the gold electrode in 10.0 μmol L^{-1} ethanolic solution of $[Cu(4\text{-mbipy-Bz-SMe})_2]^{2+}$.

Immersion time (min)	R_{CT}* (Ωcm^2)	θ	k_{app} x 10^3 (cm s^{-1})
0	17	0.0	3.13
1	60	0.72	0.888
3	70	0.76	0.761
5	78	0.78	0.683
15	75	0.77	0.710
30	73	0.77	0.730
60	71	0.76	0.750
120	76	0.78	0.701

Fig. S5 shows a series of emission spectra obtained in solution containing terephthalic acid (TA).

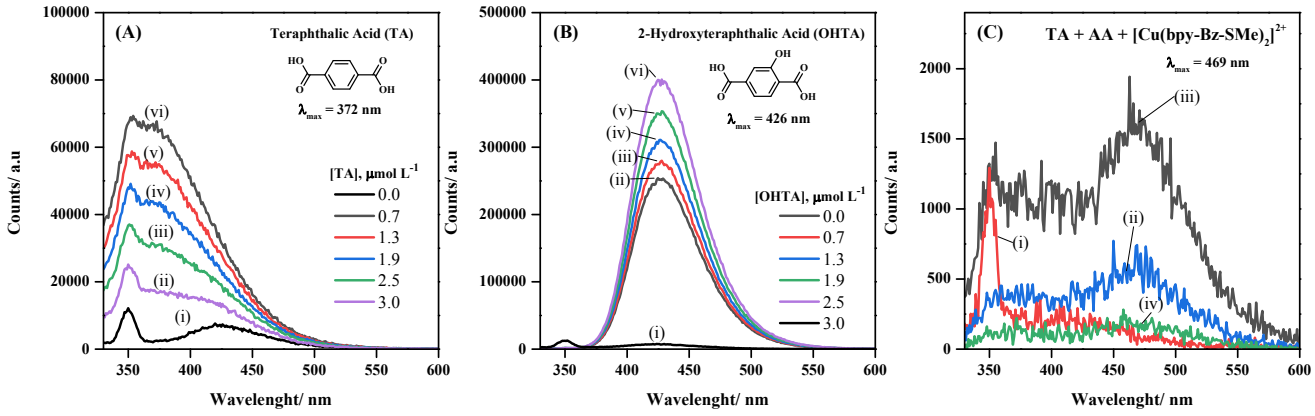

Fig. S5. Emission spectra of (A) terephthalic acid (TA) and (B) 2-hydroxyterephthalic acid (OHTA) in different concentrations in PBS 0.10 mol L^{-1}. (C) Emission spectra in PBS 0.10 mol L^{-1} (i) containing $[Cu(2CP\text{-}Bz\text{-}SMe)_2]^{2+}$ 38 μmol L^{-1} (ii), $[Cu(2CP\text{-}Bz\text{-}SMe)_2]^{2+}$ 38 μmol L^{-1} and TA 91 μmol L^{-1}, and $Cu(2CP\text{-}Bz\text{-}SMe)_2]^{2+}$ 38 μmol L^{-1}, TA 91 μmol L^{-1}, and ascorbic acid 163 μmol L^{-1}. Excitation at 312 nm.

As can be seen in in Panel (C), the spectrum obtained for the mixture of $Cu(2CP\text{-}Bz\text{-}SMe)_2]^{2+}$ with TA and ascorbic acid (curve iv) presents almost no emission probably due to an interaction between the reduced copper complex with the terephthalic acid.

Table S2 shows electrophoresis data of the DNA cleavage by a few copper complexes, including the one studied in this work.

Table S2. DNA cleavage data as obtained by agarose gel electrophoresis for some copper complexes.

Compound	[Cu] μmol L^{-1}	Reducing species/device	Incubation Time (min.)	Plasmid DNA	Degradation form	Reference
$[Cu(2CP\text{-}Bz\text{-}SMe)]^{2+}$ $[Cu(2CP\text{-}Bz\text{-}SMe)]^{2+}$	10 10	H_2AA H_2O_2	30	pBR322	Total Form II	2
$CuSO_4$ $[Cu_4(atc)_2(dien)_4(ClO_4)_2]\text{-}(ClO_4)_2{\cdot}2H_2O$	40 5, 10, and 20 40	AA^{2-}	60	pUC18	Form II Form II Forms II and III	3
$[Cu(L\text{-}Arg)_2](NO_3)_2$ [Cu(L-Arg)(phen)Cl]Cl [Cu(L-Arg)(dpq)Cl]Cl	50 10 10	Irradiation 365 nm	60	pUC19	Forms II and III Form II Forms II and III	4
$[Cu(py\text{-}phen)_2(NO_3)]NO_3$ $[Cu_2(py\text{-}phen)_2(gly)_2(NO_3)_2(H_2O)_2]{\cdot}3H_2O$ $[Cu_2(py\text{-}phen)_2(tyr)_2(H_2O)_2](NO_3)_2{\cdot}3H_2O$	0.5, 1, 2 and 4	H_2O_2	240	pUC19	Forms II and III	5
$[Cu(4\text{-}mbipy\text{-}Bz\text{-}SMe)_2]^{2+}$ $[Cu(4\text{-}mbipy\text{-}Bz\text{-}SMe)_2]^{2+}$	10	H_2AA H_2O_2	30	pBR322	Total II	This work
Results on surface						
$Au/[Cu(4\text{-}mbipy\text{-}Bz\text{-}SMe)_2]^{2+}$ (5.3×10^{-10} mol cm^{-2})		Applied potential (–0.2 V vs Ag/AgCl)	10	pBR322	Form II	This work
Fe_3O_4@Au@Cu* (0.807 mg mL^{-1})		H_2AA	30	pBR322	Form II	6

H_2AA = ascorbic acid; AA^{2-} = ascorbate; 2CP-Bz-SMe = 1,3-Bis(1',10'-phenanthrolin-2'-yloxy)-N-(4-(methylthio)benzylidene)propan-2-amine; atc = 5-amino-1,2,4-triazole-3- carboxylic acid; dien = diethylenetriamine; Arg = arginine; phen = 1,10-phenanthroline; dpq = dipyrido[3,2-2',3']-quinoxaline; py = pyridine; gly = glycine.
*Cu = $[Cu(2CP\text{-}Bz\text{-}SMe)]^{2+}$

Electrochemical study of ascorbic acid (H_2AA)

The current response of the modified surface towards the H_2AA concentration (from 0.5 to 5.0 mmol L^{-1}) was evaluated by cyclic voltammogram and is shown in Fig. S6.

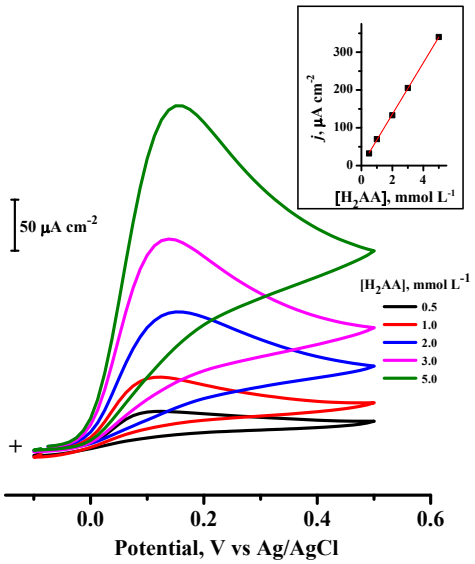

Fig. S6. Cyclic voltammograms of Au/[Cu] at 25 mV s^{-1} in 0.1 mol L^{-1} PBS (pH 7.2) containing H_2AA at different concentrations. Inset: plot of current density vs H_2AA concentration.

Fig. S7 presents the cyclic voltammograms obtained for the gold electrode modified with $[Cu(4\text{-mbpy-Bz-SMe})_2]^{2+}$ in PBS solution containing H_2AA and different concentrations of catalase. The curves presented in Fig. S7 were obtained in presence (I) and absence (II) of oxygen.

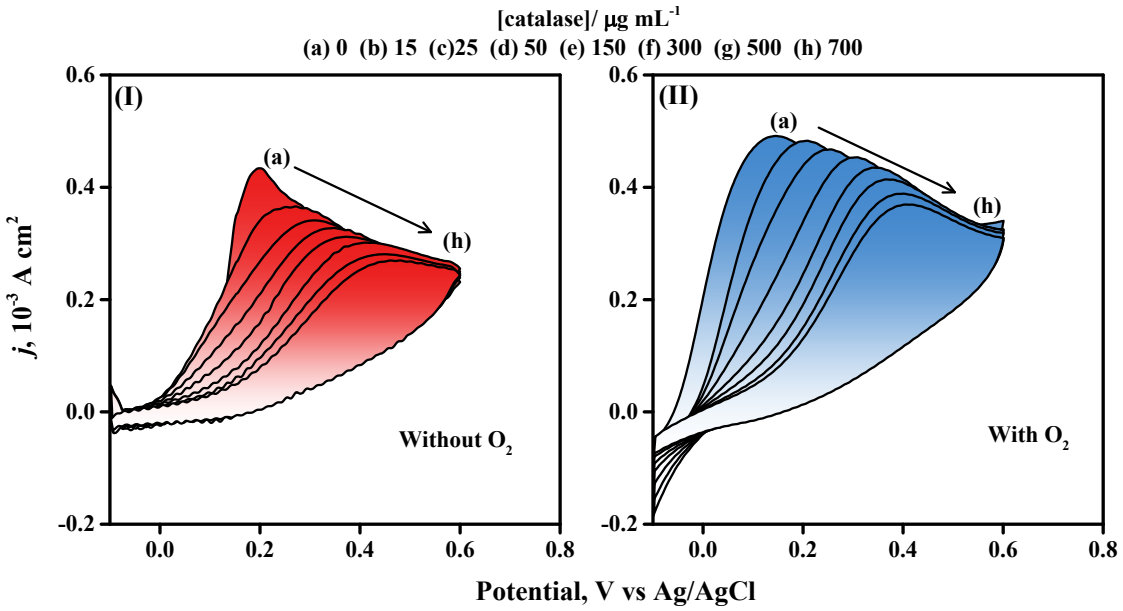

Fig. S7. Cyclic voltammograms of Au/[Cu] at 25 mV s^{-1} in 0.1 mol L^{-1} PBS containing 1.0 mmol L^{-1} H_2AA and different concentrations of catalase. The curves presented in Panels (I) and (II) were obtained in the absence (glovebox, under nitrogen atmosphere) and presence, respectively, of oxygen.

Nuclear Magnetic Resonance (NMR) spectra of (E)-1-(4'-methyl-[2,2'-bipyridine]-4-yl)-N-(4(methylthio)phenyl)methanimine (4-mbpy-Bz-SMe)

Figs S8 and S9 show the ^{1}H-NMR and ^{1}H-COSY spectra of 4-mbpy-Bz-SMe in $CDCl_3$ (400.13 MHz). Fig. S8 presents, as inset, the molecular structure with the numbering scheme for the chemical shifts assignments.

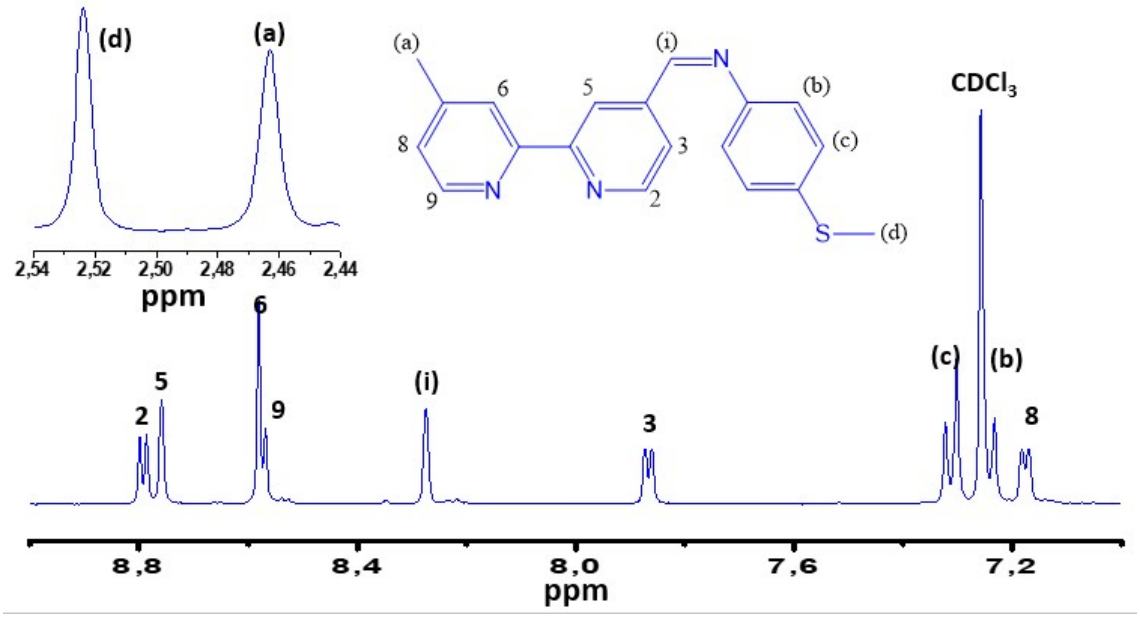

Fig. S8. ^{1}H NMR spectrum of (E)-1-(4'-methyl-[2,2'-bipyridine]-4-yl)-N-(4(methylthio)phenyl)methanimine (4-mbpy-Bz-SMe) in $CDCl_3$. Chemical shifts assignments in accordance with the numbering scheme shown in the molecular structure.

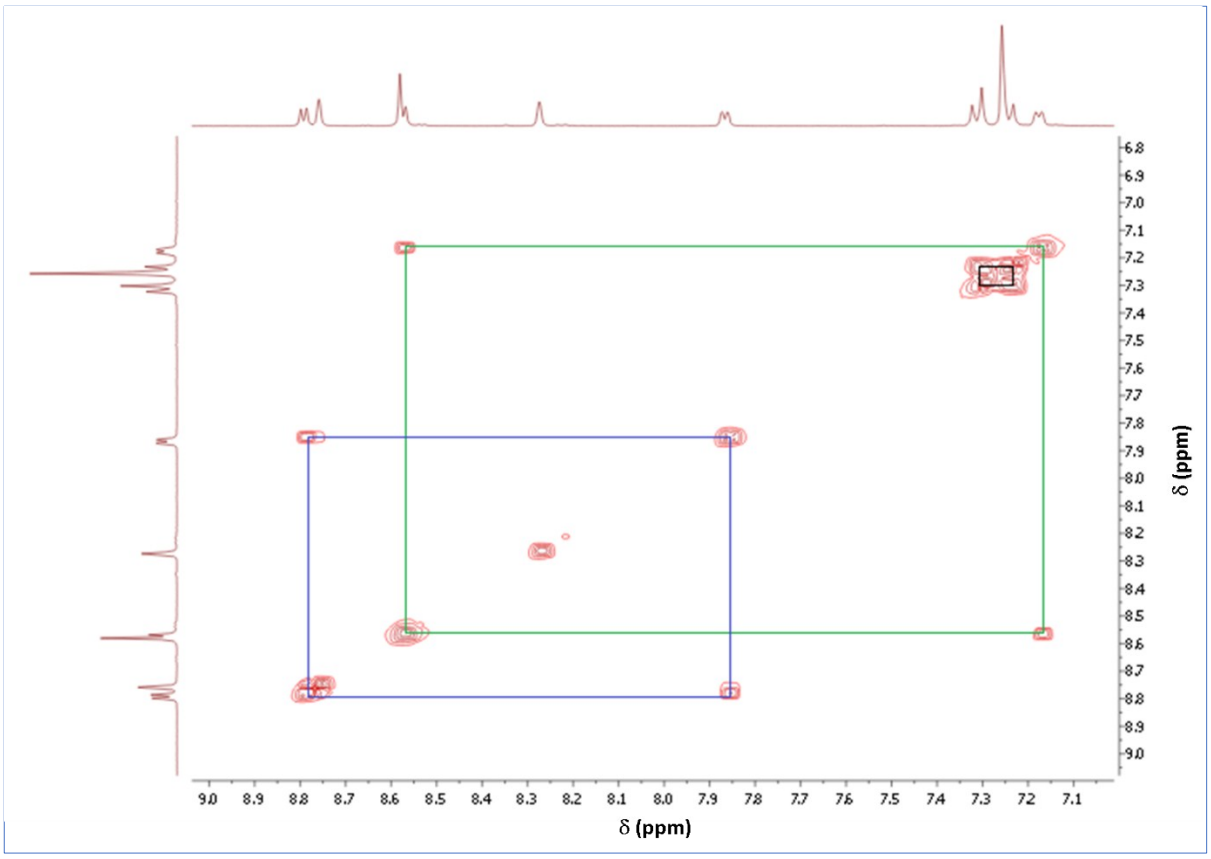

Fig. S9. ^{1}H-COSY spectrum of (E)-1-(4'-methyl-[2,2'-bipyridine]-4-yl)-N-(4(methylthio)phenyl)methanimine (4-mbpy-Bz-SMe) in $CDCl_3$.

References

1. R. A. Martinelli, G. R. Hanson, J. S. Thompson, B. Holmquist, J. R. Pilbrow, D. S. Auld and B. L. Vallee, *Biochemistry*, 1989, **28**, 2251-2258.
2. A. I. B. Romo, D. S. Abreu, T. F. Paulo, M. S. P. Carepo, E. H. S. Sousa, L. Lemus, C. Aliaga, A. A. Batista, O. R. Nascimento, H. D. Abruña and I. C. N. Diógenes, *Chem. - Eur. J.*, 2016, **22**, 10081-10089.
3. J. Hernández-Gil, S. Ferrer, A. Castiñeiras and F. Lloret, *Inorg. Chem.*, 2012, **51**, 9809-9819.
4. A. K. Patra, T. Bhowmick, S. Roy, S. Ramakumar and A. R. Chakravarty, *Inorg. Chem.*, 2009, **48**, 2932-2943.
5. L. M. Kumar, R. M. Ansari and B. R. Bhat, *Appl. Organometal. Chem.*, 2018, **32**, e4054.
6. M. A. S. Silva, A. I. B. Romo, D. S. Abreu, M. S. P. Carepo, L. Lemus, M. Jafelicci, T. F. Paulo, O. R. Nascimento, E. Vargas, J. C. Denardin and I. C. N. Diógenes, *J. Inorg. Biochem.*, 2018, **186**, 294-300.